Fish and Shellfish Immunology 94 (2019) 539–547

Contents lists available at ScienceDirect

Fish and Shellfish Immunology

journal homepage: www.elsevier.com/locate/fsi

Full length article

Northeast Chinese lamprey (*Lethenteron morii*) MyD88: Identification, expression, and functional characterization

Zebin Zhou[a,b,c], Shaoqing Ding[a,b,c], Yuanyuan He[a,b,c], Jianfeng Ren[a,b,c], Weiming Li[d], Zhang Qinghua[a,b,c,*]

[a] Key Laboratory of Exploration and Utilization of Aquatic Genetic Resources, Ministry of Education, Shanghai Ocean University, Shanghai, 201306, China
[b] International Research Center for Marine Biosciences, Ministry of Science and Technology, Shanghai Ocean University, Shanghai, 201306, China
[c] Key Laboratory of Freshwater Aquatic Genetic Resources, Ministry of Agriculture, Shanghai Ocean University, Shanghai, 201306, China
[d] Department of Fisheries and Wildlife, Michigan State University, East Lansing, MI, 48824, USA

ARTICLE INFO

Keywords:
Lamprey
Myeloid differentiation factor 88
Molecular cloning
Expression analysis
Subcellular localization

ABSTRACT

Myeloid differentiation factor 88 (MyD88) is a key adaptor of Toll-like receptors (TLR), an important pattern recognition receptor of the innate immune system. To study the origin and evolution of the vertebrate TLR signaling pathway in innate immune systems, we analyzed the biological characteristics and functions of the MyD88 gene in Northeast Chinese lamprey (*Lethenteron morii*) using PCR amplification, real-time PCR analysis, dual luciferase reporter gene assay, immunofluorescence assay, and other methods. Bioinformatics analysis showed that LmMyD88 has a modular structure consisting of Toll/IL-1R domain (TIR) and death domain (DD), which is typical of the MyD88 family. A phylogenetic tree showed that the homology of LmMyD88 was consistent with the phylogenetic status of lampreys. Tissue expression analysis indicated that the mRNA expression was expressed in some normal tissues of larval and adult *L. morii*. Real-time PCR analysis showed that the expression of LmMyD88 in tissues, such as gill and kidney, of the adult increased significantly after infection by *Pseudomonas aeruginosa*. Subcellular localization results showed that LmMyD88 was expressed in the nucleus, cytoplasm, and other parts. A dual luciferase reporter assay indicated that LmMyD88 activated nuclear factor kappa B downstream of the TLR signaling pathway. This study suggested that LmMyD88 might play an important role in the innate immune signal transduction process of *L. morii*.

1. Introduction

Pathogens that invade vertebrates are first identified by the innate immune system through various pattern recognition receptors (PRRs) [1]. Pathogens recognized by PRRs are called pathogen-associated molecular patterns (PAMP), such as bacterial lipopolysaccharide and viral double-stranded RNA [2]. PRRs recognize the pathogen and activate relevant immune cells through downstream signaling pathways, inducing immune cells to participate in inflammation and various immune responses. Toll-like receptors (TLRs) are a major family of PRRs, which can recognize various microbial components and initiate signaling pathways to induce the expression of innate immune-related genes [3]. The TLR signaling pathway is regulated by a variety of adaptor proteins containing the Toll/IL-1R (TIR) domain. The adaptor proteins that have been found so far are myeloid differentiation factor 88 (MyD88), a TIR domain-containing adaptor protein (TIRAP), TIR domain-containing adaptor inducing IFN-β (TRIF), TRIF-related adaptor molecule (TRAM), and the sterile α and armadillo-motif-containing protein (SARM) [4–7]. The TLR signaling pathway can be divided into MyD88-dependent or MyD88-independent pathways according to the adaptor proteins [8].

In mammals, TLR receptors other than TLR3 are involved in the signaling of the MyD88-dependent pathway. MyD88 acts as a key adaptor protein that participates in the signaling process of the MyD88-dependent pathway [7]. MyD88 was originally discovered in the differentiation process of myeloid cells and contains a C-terminal TIR domain and an N-terminal death domain (DD) [9]. MyD88 interacts with the TLR receptor that recognizes the pathogen through the TIR domain and then recruits and interacts with IRAK (interleukin-1 receptor-associated kinase)-4 through the DD leading to IRAK1 phosphorylation by IRAK4. Activated IRAK-1 associates with and further phosphorylates TNF receptor-associated factor (TRAF) 6, thereby

* Corresponding author. Key Laboratory of Exploration and Utilization of Aquatic Genetic Resources, Ministry of Education, Shanghai Ocean University, Shanghai, 201306, China. Tel.: +86 21 61900456.
E-mail address: qhzhang@shou.edu.cn (Q. Zhang).

https://doi.org/10.1016/j.fsi.2019.09.035
Received 11 July 2019; Received in revised form 5 September 2019; Accepted 14 September 2019
Available online 15 September 2019

activating downstream transcription factor activator protein (AP)-1 signaling and the transcription factor nuclear factor kappa B (NF-κB) signaling pathway which ultimately regulates the expression of inflammatory cytokines and growth factors [10,11].

MyD88 has been found in several species since it was first cloned in mice in 1990 [9], such as *Homo sapiens* [12], *Gallus gallus* [13], *Xenopus laevis* [14], and others. Similarly, MyD88 is known to be found in *Danio rerio* [15], *Paralichthys olivaceus* [16], *Oncorhynchus mykiss* [17], *Salmo salar* [18], *Miichthys miiuy* [19], and other teleost species. Sequence analysis showed that MyD88 is highly conserved among different species and has a TIR domain and DD in fish, amphibians, birds, and mammals. The results suggest that fish MyD88 may have similar functions and characteristics as mammals. However, the specific mechanism of MyD88 and its involvement in the immune signaling pathways of primitive vertebrates remains to be resolved.

Northeast Chinese lamprey (*Lethenteron morii*) is one of the extant jawless vertebrates that belong to Cyclostomata, Petromyzontiformes, *Petromyzontidae*, and *Lampetra*. They are classified as Agnatha, which are evolutionary more primitive than fish. As the oldest vertebrate group, *Lampetra* are the bridge between invertebrates and vertebrates. A study has found that modern *Lampetra* have not changed that much from its ancestors of 360 million years ago and is one of the few living fossils [20]. As lampreys are the ancestors of vertebrates, studying the mechanism of their innate immune system can provide an important reference for the origin and evolution of innate immunity. Multiple TLRs have been identified in *Petromyzon marinus* and *Lampetra japonicum* [21], and MyD88-dependent pathway-associated proteins have been found in *Lampetra japonicum* [22]. However, the specific signaling mechanism of the lamprey MyD88-dependent pathway is not yet clear. In this study, the MyD88 gene of *L. morii* was first cloned, and its molecular structure and expression in tissues and cell localization were further explored. LmMyD88 was found to promote the activity of the NF-κB promoter by luciferase reporter gene assay, which laid the foundation for the *L. morii* MyD88 signaling pathway research.

2. Materials and methods

2.1. Sample collection and bacteria

This research used healthy *L. morii* from tributaries of the Yalu River in Dandong City, Liaoning Province, China. They were temporarily bred in a water temperature of 8 ± 1 °C. The average body length of larvae was 11.5 ± 0.8 cm, and the body weight was 5.2 ± 0.6 g. The average body length of adults was 30.1 ± 3.2 cm, and the body weight was 36.1 ± 2.1 g.

Pseudomonas aeruginosa PA11 strain, which was isolated from diseased *L. morii* and stored at −80 °C in our laboratory, was used to challenge the healthy larvae and adult lampreys.

2.2. Northeast Chinese lamprey (L. morii) RNA extraction and cDNA synthesis

Three healthy larvae and adult Northeast Chinese lamprey (*L. morii*) and nine tissues including brain, intestine, heart, gill, liver, muscle, kidney, supraneural body, and skin were selected for this study. The Trizol (Invitrogen, Carlsbad, CA, USA) method was used to extract total RNA from *L. morii* and RNA samples using 1% agarose gel electrophoresis validation and spectrophotometry (NanoDrop, Thermo Scientific, USA) to assess sample concentration and stored at −80 °C. Northeast Chinese lamprey adults received an abdominal cavity injection (500 μL/100 g) of *P. aeruginosa* (1.96×10^6 CFU/mL). Total RNA was extracted from the supraneural body, gill, intestine and kidney at 0, 6, 12, 24, 48, 72 h and stored at −80 °C. RNA samples were reverse transcribed into cDNA using the PrimeScriptTM RT reagent kit with gDNA Eraser (Takara Bio, Beijing, China), and the actual procedure was performed according to the kit instructions.

2.3. LmMyD88 clone and sequence analysis

The preliminary sequence of MyD88 was obtained from the transcriptome data of closely related species, such as *Lampetra japonica* (http://jlampreygenome.imcb.a-star.edu.sg/) and *Petromyzon marinus* (https://genomes.stowers.org/organism/Petromyzon/marinus) by BLAST. The open reading frame (ORF) sequence of MyD88 was cloned using MyD88-F/R primers designed by using highly conserved MyD88 sequence from species of Agnatha vertebrates (STable.1). The primers were synthesized by Sangon Biotech Co., Ltd. (Shanghai, China).

PCR amplification was performed using mixed cDNA of healthy tissue from *L. morii* as a template. The PCR system (25 μL) was as follows: DNA polymerase 12.5 μL, ddH_2O 9.5 μL, MyD88-F 1.0 μL, MyD88-R 1.0 μL, and cDNA 1.0 μL. The PCR conditions were as follows: predenaturation at 98 °C for 2 min; denaturation at 98 °C for 30 s, annealing at 58 °C for 30 s, extension at 72 °C for 1 min, amplification for 35 cycles; extension at 72 °C for 5 min, storage at 12 °C. The PCR product was detected by 2% agarose gel electrophoresis, and the target fragment was purified by a DNA Fragment Purification Kit (Takara Bio). The target fragment was ligated into a pMD-19T vector and transformed into competent bacteria DH5α (Tiangen, Beijing, China), which were screened for blue/white colonies. After PCR identification, the positive clones were sent to Sangon Biotech Co., Ltd for sequencing. Homologous sequence was identified using the BLASTP tool from NCBI (http://www.ncbi.nlm.nih.gov/BLAST); Getorf software (http://emboss.bioinformatics.nl/cgi-bin/emboss/getorf) was used to predict ORFs; ExPASy software (http://web.expasy.org/protparam/) was used to predict the relative mass and theoretical isoelectric point; SMART software (http://smart.embl-heidelberg.de/) was used to predict and analyze protein domains; SignalP 4.1 software (http://www.cbs.dtu.dk/services/SignalP/) was used to predict protein signal peptides; TMHMM software (http://www.cbs.dtu.dk/services/TMHMM-2.0/) was used to predict protein domains; PROSITE software (http://prosite.expasy.org/) was used to predict protein subcellular localization; ClustalX 2.0 software was used to align multiple protein sequences; MEGA 7.0 software and iTOL software (http://itol.embl.de/) were used to build a phylogenetic tree.

2.4. Expression of LmMyD88 in tissues of L. morii

Real-time PCR was used to detect the expression of MyD88 in different tissues and adults of *L. morii* after *P. aeruginosa* infection. β-actin was used as a reference gene (SFig. 1) with the primers β-actin-qF and β-actin-qR; MyD88-qF and MyD88-qR were designed as MyD88 specific primers (STable 1). The primers were synthesized by Sangon Biotech Co., Ltd. The real-time PCR reaction was carried out using a LightCycler 480 II real-time PCR machine. The real-time PCR reaction system was as follows: Master Mix (Takara Bio) 10.0 μL, ddH_2O 7.0 μL, upstream primer 1.0 μL, downstream primer 1.0 μL, and cDNA 1.0 μL. The real-time PCR reaction conditions were as follows: 50 °C for 2 min, 95 °C for 10 min; 95 °C for 10 s, 60 °C for 30 s, amplification for 40 cycles; 95 °C for 30 s, 60 °C for 30 s, 40 °C for 30 s. Each sample was repeated three times, and the relative expression of LmMyD88 was calculated by using the $2^{-\Delta\Delta CT}$ method. The results were expressed as the mean ± standard error of the mean (SEM), and significant difference analysis was performed with SPSS 19.0 software. $P < 0.05$ indicates significant differences.

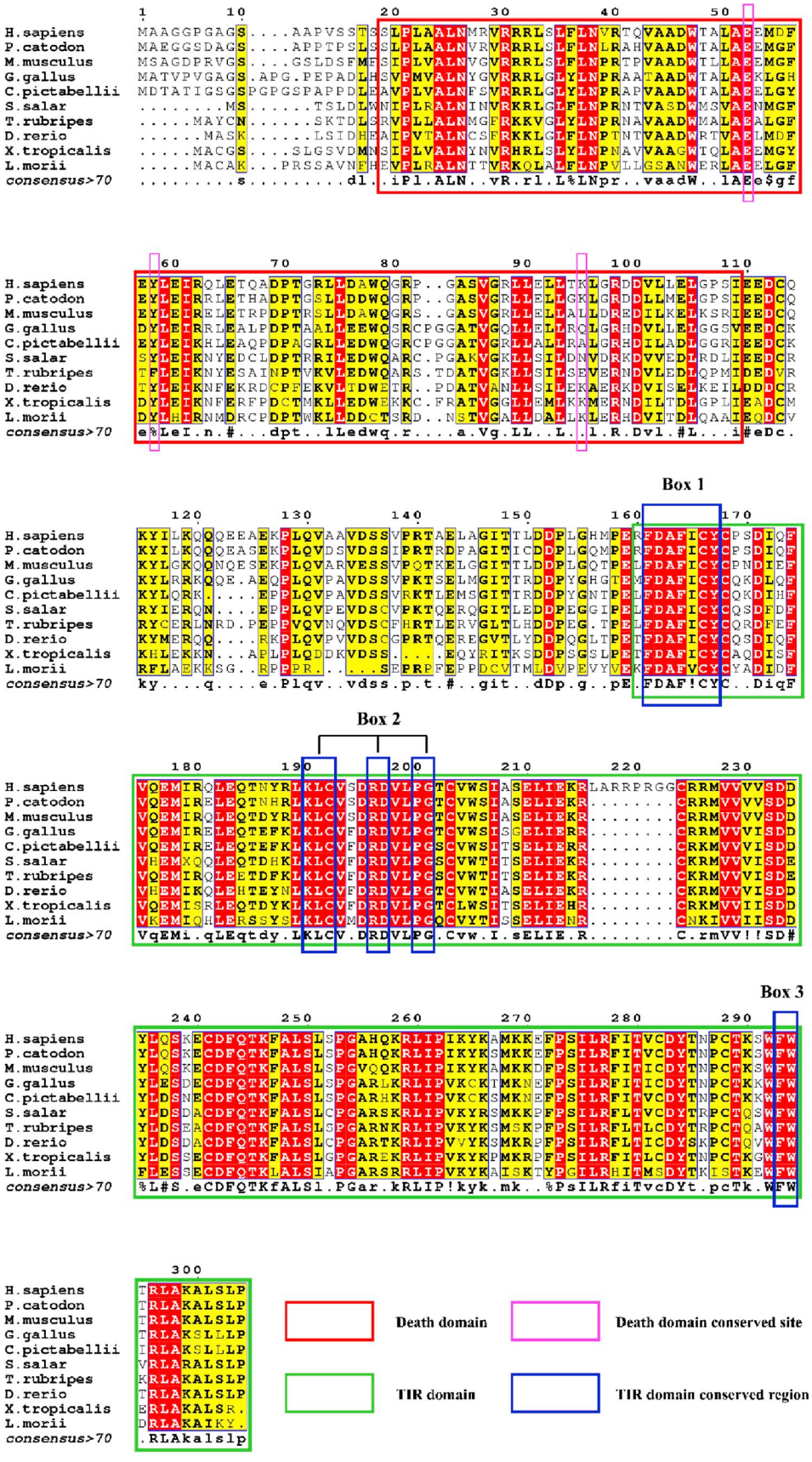

Fig. 1. Multiple sequence alignment of *L. morii* MyD88 with other species MyD88.
The multiple sequence alignment is based on MyD88 sequences from *Homo sapiens* (accession number NP_001166038.2), *Mus musculus* (accession number NP_034981.1), *Gallus gallus* (accession number NP_001026133.2), *Chrysemys picta bellii* (accession number XP_005297196.1), *Xenopus tropicalis* (accession number NP_001016837.1), *Danio rerio* (accession number NP_997979.2), *Salmo salar* (accession number NP_001130017.1), *Takifugu rubripes* (accession number NP_001106666.1), *Physeter catodon* (accession number XP_007127842.1), and *L. morii* (accession number AYP27510.1).

a

Percent Identity

1 LM	100.00									
2 DR	47.45	100.00								
3 SS	50.00	69.86	100.00							
4 TR	49.46	67.49	73.76	100.00						
5 XT	54.24	61.01	62.32	60.71	100.00					
6 MM	49.82	60.78	64.06	59.79	65.48	100.00				
7 HS	50.18	61.13	63.70	60.14	64.41	81.76	100.00			
8 PC	49.47	60.07	63.70	60.14	64.77	78.38	88.85	100.00		
9 GG	50.53	59.72	62.90	61.32	64.54	68.84	70.55	68.84	100.00	
10 CP	50.90	61.57	67.26	66.08	68.57	69.66	70.34	70.34	79.66	100.00
	1 LM	2 DR	3 SS	4 TR	5 XT	6 MM	7 HS	8 PC	9 GG	10 CP

b

Death Domain Percent Identity

1 LM	100.00									
2 XT	51.11	100.00								
3 MM	47.25	57.78	100.00							
4 HS	46.15	54.44	74.43	100.00						
5 PC	47.25	57.78	75.82	86.81	100.00					
6 GG	48.35	56.52	62.64	63.74	64.84	100.00				
7 CP	48.35	60.87	67.03	65.93	67.03	73.12	100.00			
8 DR	42.22	46.15	45.56	44.44	43.33	41.76	45.05	100.00		
9 SS	46.67	52.17	55.56	52.22	52.22	50.00	55.43	54.95	100.00	
10 TR	47.78	51.90	47.78	48.89	48.89	52.17	54.35	54.95	60.87	100.00
	1 LM	2 XT	3 MM	4 HS	5 PC	6 GG	7 CP	8 DR	9 SS	10 TR

c

TIR Domain Percent Identity

1 LM	100.00									
2 DR	62.50	100.00								
3 SS	61.76	83.94	100.00							
4 TR	62.50	82.48	88.32	100.00						
5 HS	63.24	78.83	75.91	76.64	100.00					
6 PC	62.22	78.68	77.21	77.21	97.81	100.00				
7 MM	62.96	77.94	75.74	78.68	94.16	91.97	100.00			
8 XT	66.18	77.94	75.74	77.94	78.68	78.52	79.26	100.00		
9 GG	62.50	78.10	74.45	77.37	81.02	82.35	80.15	78.68	100.00	
10 CP	63.24	76.84	78.10	81.02	80.29	82.35	79.41	81.62	90.51	100.00
	1 LM	2 DR	3 SS	4 TR	5 HS	6 PC	7 MM	8 XT	9 GG	10 CP

Fig. 2. Similarity between the amino acid sequence of *L. morii* MyD88 and the MyD88 of other species. (a) Similarity comparison based on the sequences of MyD88 from *Homo sapiens* (accession number NP_001166038.2), *Mus musculus* (accession number NP_034981.1), *Gallus gallus* (accession number NP_001026133.2), *Chrysemys picta bellii* (accession number XP_005297196.1), *Xenopus tropicalis* (accession number NP_001016837.1), *Danio rerio* (accession number NP_997979.2), *Salmo salar* (accession number NP_001130017.1), *Takifugu rubripes* (accession number NP_001106666.1), *Physeter catodon* (accession number XP_007127842.1), and *L. morii* (accession number AYP27510.1). (b) Comparison of MyD88 death domains in *H. sapiens* (accession number NP_001166038.2), *M. musculus* (accession number NP_034981.1), *G. gallus* (accession number NP_001026133.2), *C. picta bellii* (accession number XP_005297196.1), *X. tropicalis* (accession number NP_001016837.1), *D. rerio* (accession number NP_997979.2), *S. salar* (accession number NP_001130017.1), *T. rubripes* (accession number NP_001106666.1), *P. catodon* (accession number XP_007127842.1), and *L. morii* (accession number AYP27510.1). (c) Comparison of MyD88 TIR domains in *H. sapiens* (accession number NP_001166038.2), *M. musculus* (accession number NP_034981.1), *G. gallus* (accession number NP_001026133.2), *C. picta bellii* (accession number XP_005297196.1), *X. tropicalis* (accession number NP_001016837.1), *D. rerio* (accession number NP_997979.2), *S. salar* (accession number NP_001130017.1), *T. rubripes* (accession number NP_001106666.1), *P. catodon* (accession number XP_007127842.1), and *L. morii* (accession number AYP27510.1).

2.5. LmMyD88 subcellular location

Amplification of the LmMyD88 gene fragment without the stop codon (TGA) using the upstream primer containing the *Bam*HI restriction site and the downstream primer containing the *Hin*dIII restriction site. The target fragment was double-digested with the corresponding restriction endonuclease, and T4 ligase was used to connect to the pCMV-tag 2B eukaryotic expression vector that could be expressed in mammalian cells. The ligation product was transformed into competent DH5α bacteria cells, positive clones were selected, and the recombinant plasmid was subjected to double enzyme digestion for verification.

HEK293T cells were seeded in 35 mm glass bottom culture dish at 2×10^5 cells per 24 h before transfection and then transfected at a cell fusion rate of 60%–70%. pCMV-LmMyD88 and pCMV empty plasmid were transfected 500 ng per culture dish with Fugene® HD transfection reagent (Promega, Madison, WI, USA). Cells were fixed with 4% paraformaldehyde after transfection for 24 h, rinsed three times with 1 × PBS, and permeabilized with 100% methanol at −20 °C. The samples were incubated after rinsing with 1 × PBS in blocking buffer (1 × PBS/5% normal goat serum/0.3% Triton X-100) for 1 h. After blocking, antibody buffer was added [1 × PBS/1% BSA/0.3% Triton X-100/1:100 PDI Rabbit mAb or 1:400 AIF XP Rabbit mAb (Cell Signaling Technology, Danvers, MA, USA)/1:1,000 Monoclonal ANTI-FLAG® M2 antibody produced in mouse (Sigma-Aldrich, St. Louis, MO, USA)]. The

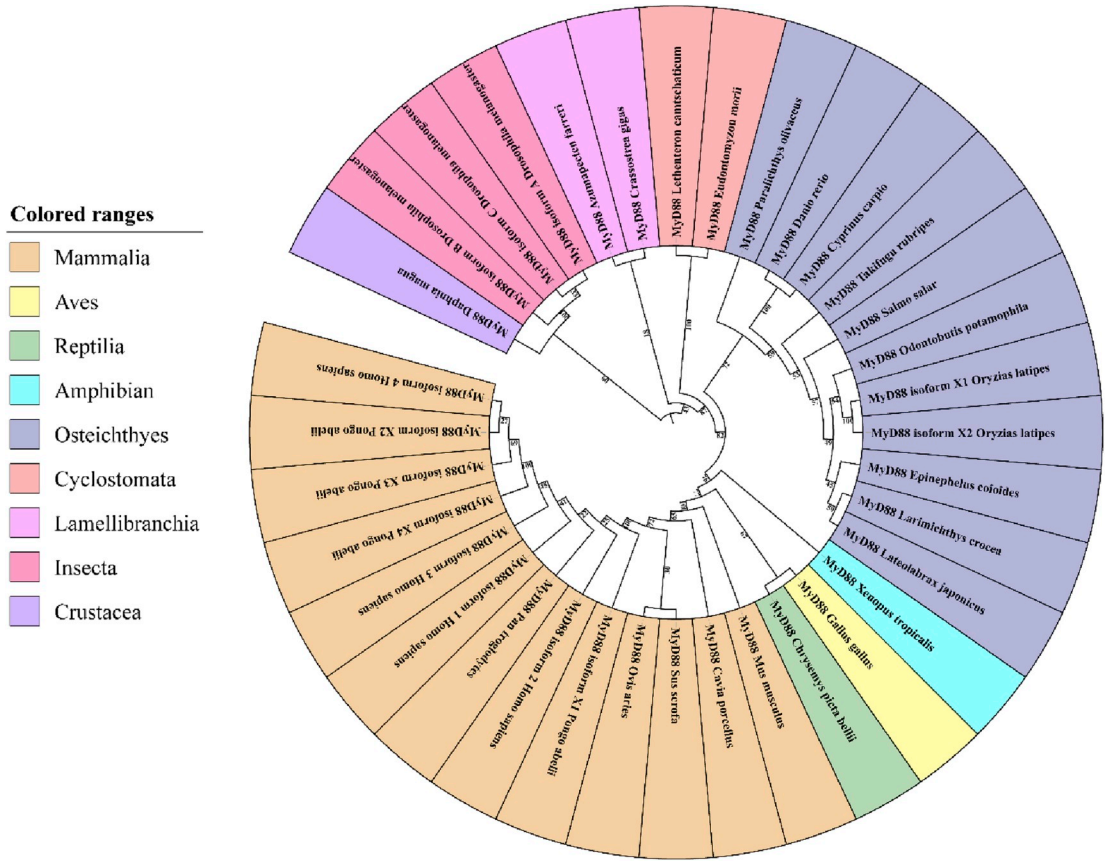

Fig. 3. Neighbor-joining method to construct a MyD88 phylogenetic tree. The sequences used to construct the phylogenetic tree are shown in STable 2. The bootstrap value is set to 1,000.

secondary anti-buffer buffer containing the coupled fluorescein secondary antibody [goat anti-mouse IgG (H + L) cross-adsorbed secondary antibody, Alexa Fluor 488/goat anti-rabbit IgG (H + L) cross-adsorbed secondary antibody, Alexa Fluor 594 (Invitrogen)] and the Hoechst 33342 nuclear stain (Solarbio, Beijing, China) was prepared by adding the antibody dilution buffer (1 × PBS/1% BSA/0.3% Triton X-100), and the specimen was incubated for 1–2 h at room temperature in the dark. After rinsing three times in 1 × PBS, the specimen was observed under a confocal microscope and photographed.

2.6. Luciferase analysis

In order to study the effect of MyD88 on NF-κB activity, we cloned NF-κB promoter from *L. morii* by homologous sequence comparison, and constructed pGL3-NF-κB promoter reporter gene (accession number MN368861) HEK293T cells were seeded in 24-well plates at 5×10^4 cells per well 24 h before transfection and then transfected at a cell fusion rate of 70%–80%. Transfection was performed according to the instructions of the Fugene® HD kit. Seven groups were set up and each group was transfected with pCMV-LmMyD88 0 (control group), 50, 100, 150, 200, 250, and 300 ng. The transgenic amount of the *L. morii* NF-κB promoter was 100 ng. The phRL-TK reference plasmid was added in a ratio of 10:1. The remainder of the system was complemented with pCMV empty plasmid. After transfection for 24 h, the dual luciferase reporter gene assay was performed according to the Dual Luciferase® Reporter Assay System (Promega) instructions. Three sets of technical replicates were performed in each group, and the experiment was repeated three times. The results were expressed as the mean ± SEM, and significant difference analysis was performed using SPSS 19.0 software, $P < 0.05$ indicates a significant difference, $P < 0.01$ indicates a highly significant difference.

2.7. Key resource table

Resource	Source	Identifier
Antibodies		
PDI (C81H6) Rabbit mAb	Cell Signaling Technology	AB_2156433
AIF (D39D2) XP Rabbit mAb	Cell Signaling Technology	AB_10634755
Monoclonal ANTI-FLAG® M2 antibody	Sigma-Aldrich	AB_262044
Goat anti-Mouse IgG (H + L) Cross-Adsorbed Secondary Antibody, Alexa Fluor 488	Invitrogen	AB_2534069
Goat anti-Rabbit IgG (H + L) Cross-Adsorbed Secondary Antibody, Alexa Fluor 594	Invitrogen	AB_2534079
Chemical		
Normal Goat Serum	Jackson	
Bovine Serum Albumin (BSA)	Sigma-Aldrich	
Paraformaldehyde	Sigma-Aldrich	
Hoechst 33342	Solarbio	
Methanol	Sangon	
20× PBS Solution	Sangon	
Triton X-100	Sangon	

3. Results

3.1. Molecular cloning and sequence analysis of LmMyD88

The ORF of LmMyD88 gene was 852 bp, encoding 283 amino acids (SFig. 2). The relative molecular mass was 32.432 kD and the

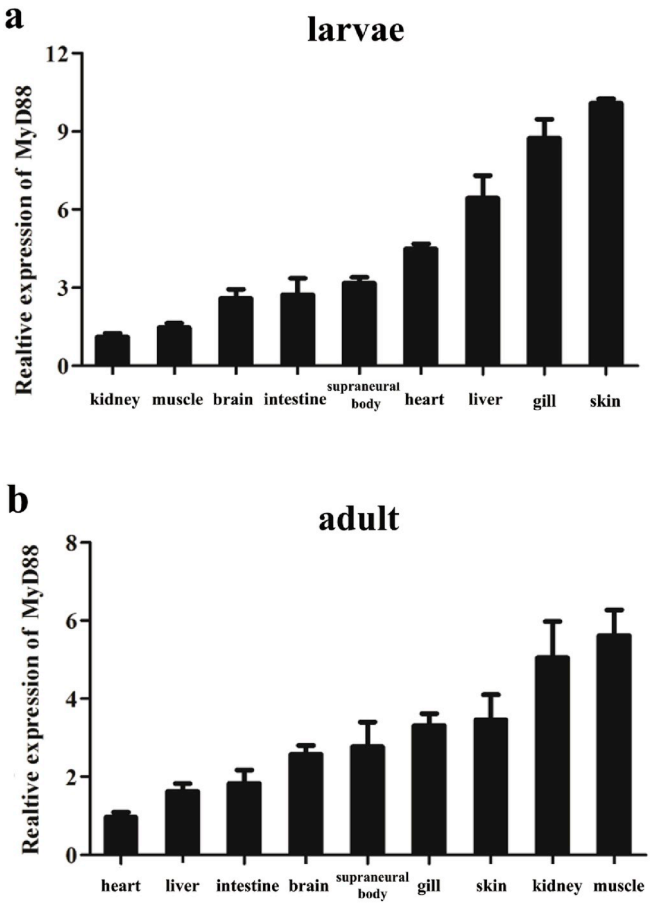

Fig. 4. Relative expression of *L. morii* MyD88 in different tissues of larvae and adults. *L. morii* MyD88 relative expression in the brain, intestine, heart, gill, liver, muscle, kidney, supraneural body, and skin of (a) the larvae and (b) the adults. The relative expression was calculated by the $2^{-\Delta\Delta CT}$ method, β-actin was used as the reference gene, and the experimental results were expressed as mean ± standard error (SEM), *Indicates a significant difference compared with the control group ($n = 3$, $P < 0.05$).

theoretical isoelectric point was 6.25 with no signal peptide and transmembrane domain. The sequence was submitted to GenBank (access number AYP27510.1). The SMART predictive analysis of the MyD88 protein domain revealed that the sequence contains typical domains of the MyD88 protein: the N-terminal DD (15–105 aa) and the C-terminal TIR domain (148–282 aa) (SFig. 3). PSORT II software predicted and analyzed the subcellular localization of MyD88 which showed that MyD88 protein occurred at 34.8% in the cytoplasm, 30.4% in the mitochondria, and 26.1% in the nucleus.

3.2. Multiple sequence alignment and phylogenetic tree analysis of LmMyD88

Sequence alignment between LmMyD88 and the MyD88 of other vertebrates showed that the Death domain and TIR domain existed in all species. The modular structure of LmMyD88 contains three DD conserved sites (E48A, Y54A, K91A) and three TIR domain conserved regions (box1 (^{149}FDAFVCY^{155}), box2 (^{178}KLC-RD-PG^{189}), box3 (^{273}FW^{274})) (Fig. 1). The similarity of MyD88 amino acid sequence between *L. morii* and other species was 47%–54%, of which the similarity of the DD domain was 42%–51%, and that of the TIR domain was 61%–66% (Fig. 2). The phylogenetic tree showed that the MyD88 of Mammalia, Aves, and Reptilia were clustered on a branch, Osteichthyes was clustered on a branch, and lampreys and other vertebrates were clustered on a big branch. Meanwhile, MyD88 had a high homology between lampreys and Osteichthyes. The phylogenetic tree of MyD88 was in line with the evolutionary position of species, and MyD88 of *L. morii* was between vertebrates and invertebrates (Fig. 3).

3.3. Expression of LmMyD88 in tissues of L. morii

Real-time PCR analysis results showed that LmMyD88 was expressed in the heart, brain, muscle, skin, gill, intestine, liver, supraneural body, and kidney of larvae and adult *L. morii*. The expression of LmMyD88 was relatively high in the skin, gill, and liver of larvae *L. morii*, but relatively low in the kidney and muscle. LmMyD88 was expressed relatively highly in the kidney and muscle of adult *L. morii* (Fig. 4).

Real-time PCR analysis was used to detect the expression level of LmMyD88 in different tissues at different times after infection by *P. aeruginosa*. The results showed that after *P. aeruginosa* infection, the expression level of MyD88 in adults showed an increasing trend from 0 to 48 h, and reached a peak at 48 h, which was significantly different from that at 0 h ($P < 0.05$). The expression level of MyD88 in the intestine of *L. morii* increased after 72 h, but there was no significant difference compared with 0 h ($P > 0.05$). The expression level of MyD88 in the gill was significantly increased at 12 h and 72 h, and significantly different from that at 0 h ($P < 0.05$). The expression level of MyD88 in the kidney was significantly increased at 24 h compared with 0 h ($P < 0.05$). After 24 h, the expression level of LmMyD88 gradually decreased and tended to be stable (Fig. 5).

3.4. LmMyD88 cell localization

The results of cellular immunofluorescence confirmed the location of LmMyD88 in cells. Under confocal microscopy, LmMyD88 was clustered in HEK 293T cells and expressed in the nucleus and cytoplasm. However, although LmMyD88 overlapped with markers of mitochondria and endoplasmic reticulum, it had no specific co-localization with these markers (Fig. 6).

3.5. Overexpression of LmMyD88 on NF-κB promoter activity

The results of the dual luciferase reporter assay showed that the activity of the NF-κB promoter in *L. morii* was significantly increased compared with the control group after transfection with pCMV-LmMyD88 ($p < 0.01$), and with increments of pCMV-LmMyD88 transfection, NF-κB promoter activity increased slightly. However, when the pCMV-LmMyD88 transfection was greater than 200 ng the NF-κB promoter activity was not affected (Fig. 7).

4. Discussion

Northeast Chinese lamprey is one of the oldest Agnatha, therefore, studies of the immune system in this species could reveal the origins of the early immune system. This study found that LmMyD88 has an ORF of 852 bp, encoding 283 amino acids. Alignment with sequences from other species showed that LmMyD88 had a conserved DD and TIR domain. Though LmMyD88 was less similar to other vertebrates (the DD is relatively less similar than the TIR domain), it had multiple conserved regions. In the typical MyD88-dependent pathway, the TIR domain of MyD88 binds to the TIR domain of the TLR. Specifically, box1 and box2 are involved in the signaling binding sites in TLR signaling pathway, whereas box3 is involved in directing the protein localization [23]. After the upstream interaction, MyD88 recruits downstream IRAK4 and other linker molecules through the DD for further signaling. However, the defect of MyD88 DD conserved sites can affect the recruitment of IRAK1 and IRAK4 [24]. Combining domain sequence alignment results, it is speculated that the further signaling mechanism of MyD88 in *L. morii* after binding to TLR might be similar to other vertebrates. The results of the phylogenetic tree were consistent with the evolutionary

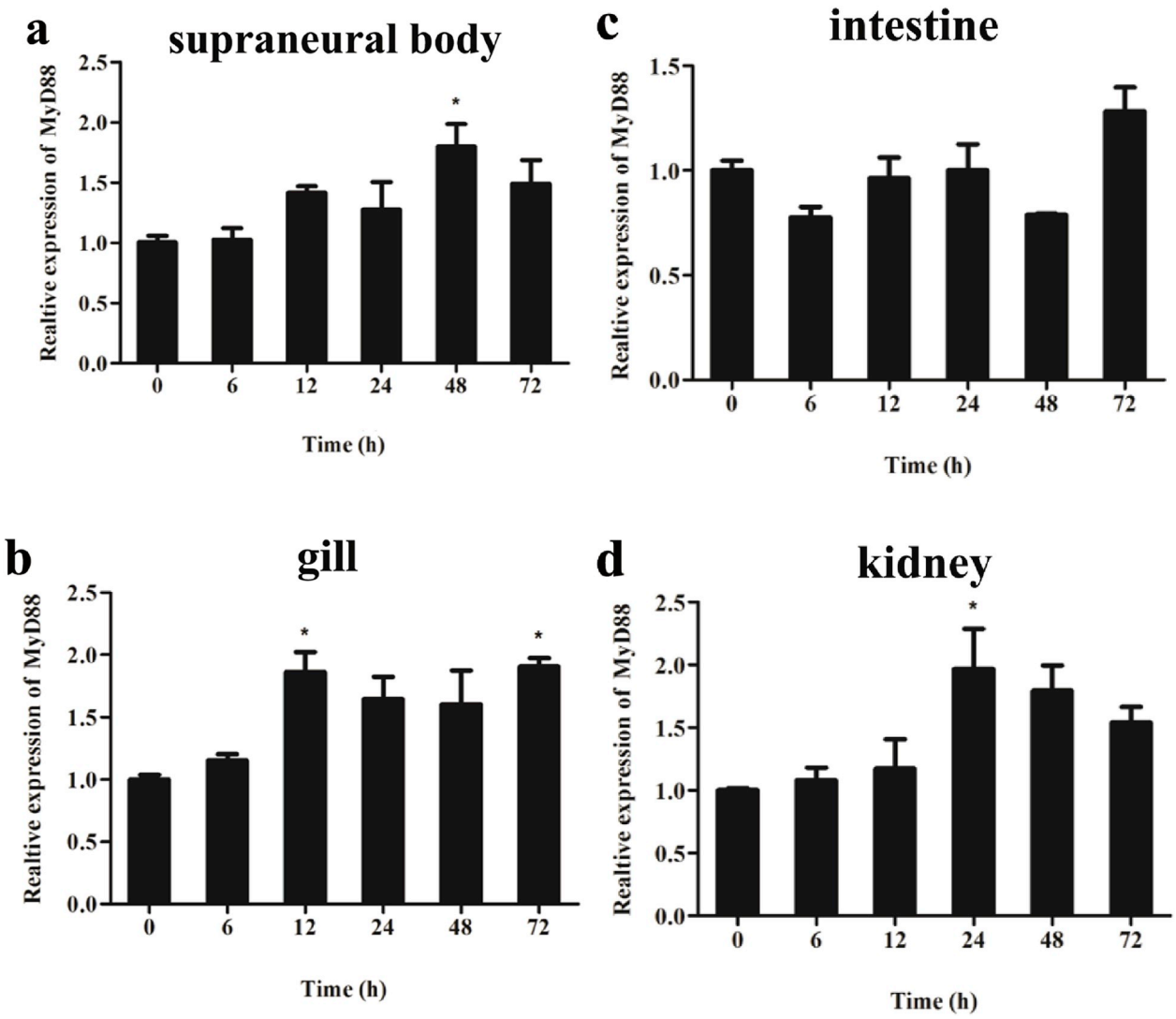

Fig. 5. Changes in the expression of *L. morii* MyD88 in various tissues after *Pseudomonas aeruginosa* infection. Relative expression of MyD88 in (a) the supraneural body, (b) gill, (c) intestine, and (d) kidney of *L. morii* adults after *P. aeruginosa* infection at 0, 6, 12, 24, 48, and 72 h. The relative expression was calculated by the $2^{-\Delta\Delta CT}$ method, β-actin was used as the reference gene, and the experimental results were expressed as mean ± standard error (SEM), *Indicates a significant difference compared with the control group ($n = 3$, $P < 0.05$).

status of the species. Previous studies have shown that fish and mammalian MyD88 are more conservative in evolution, which was consistent with the results of the phylogenetic tree analysis [25]. Multiple sequence alignments and phylogenetic tree results indicated that Northeast Chinese lamprey had certain specificity compared with higher vertebrate animals.

The results of tissue expression analysis showed that LmMyD88 was expressed in the larval and adult tissues of Northeast Chinese lamprey, which was consistent with the expression of MyD88 in other species. However, the tissue expression profiles of MyD88 in different species were not the same. For example, in *Pelteobagrus fulvidraco*, MyD88 has the highest expression in the spleen and the lowest expression in the intestine [26]; duck MyD88 has the highest expression in the spleen but expression is relatively low in muscle and liver [27]. Moreover, the relative expression of MyD88 is also different in different genders of the same species. In female *Sepiella japonica*, MyD88 has the highest expression in the ovary and the lowest expression in the brain; while the male MyD88 has the highest expression in the gill and the lowest expression in the optic lobe [28]. This study showed that LmMyD88 was relatively high in the skin, gill, and liver of Northeast Chinese lamprey larvae, but relatively low in kidney and muscle. The expression of LmMyD88 in the kidney and muscle of Northeast Chinese lamprey were relatively high, and the expression in the heart was relatively low. The MyD88 relative expression of different species in tissues may be related to specific differences, sex differences, and different growth stages. For example, in this study, the Northeast Chinese lamprey larvae were in the developmental stage, and the adults were in the reproductive stage. On the whole, MyD88 was expressed in different tissues of basal vertebrates.

Previous studies have shown that MyD88 is widely involved in the innate immune response to pathogens such as bacteria and viruses. *Patinopecten yessoensis* MyD88 has significant expression 3–6 h after infection with Gram-positive and Gram-negative bacteria [29]. *Artemia sinica* MyD88 was significantly upregulated after a bacterial challenge [30]. Also in fish, *Anguilla japonica* MyD88 was significantly increased in the head-kidney, spleen, and other tissues after 8 h of infection with *E. tarda*. The expression level of MyD88 in the head-kidney and spleen was significantly increased after stimulation with a double-stranded RNA analogue poly I:C for 16–24 h [31]. The *P. aeruginosa* used in this study belonged to Gram-negative bacteria. In the typical innate immune recognition mode, the lipopolysaccharide in the outer structure of the cell wall can be recognized by Toll-like receptors and further stimulate

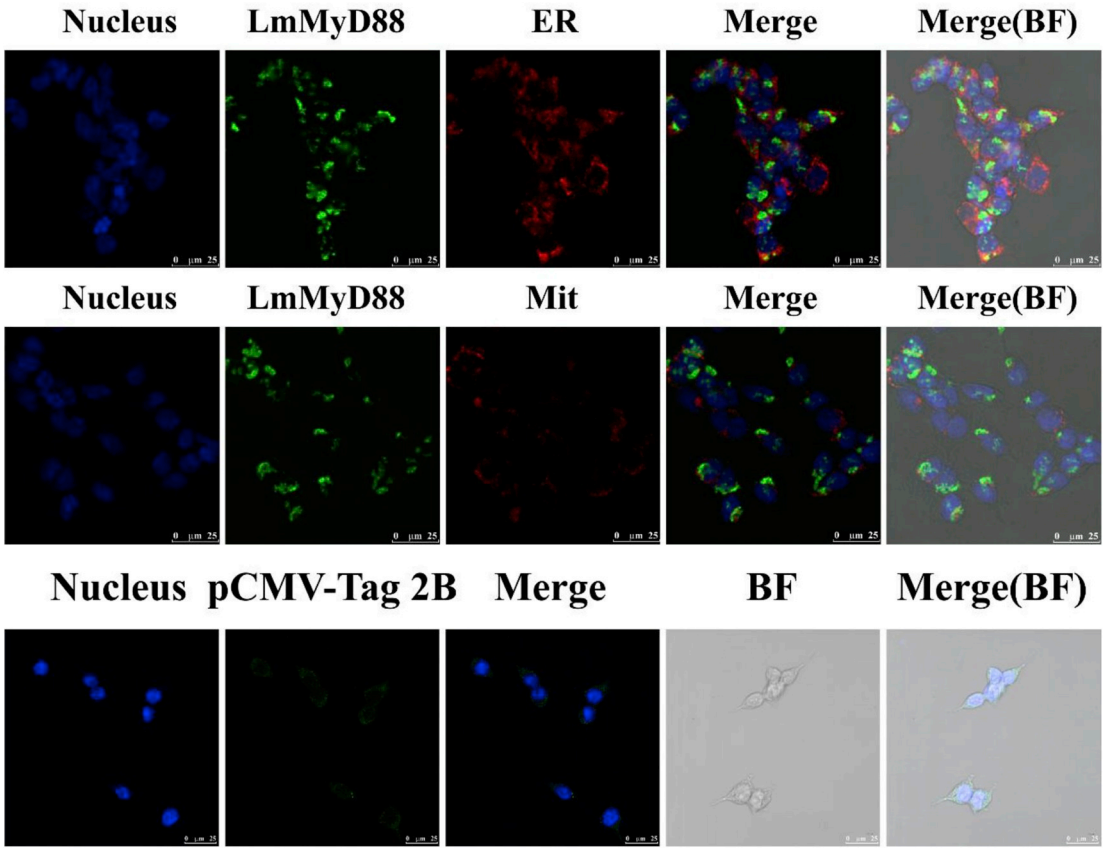

Fig. 6. Localization of LmMyD88 in HEK293T cells.
DAPI stained nuclei (blue fluorescence), FLAG-tagged antibody labeled pCMV-MyD88 fusion protein (green fluorescence), endoplasmic reticulum and mitochondria are marked with red fluorescence, and bright field observations. Empty plasmid (pCMV) was used as a control, the scale is shown in the figure. . (For interpretation of the references to colour in this figure legend, the reader is referred to the Web version of this article.)

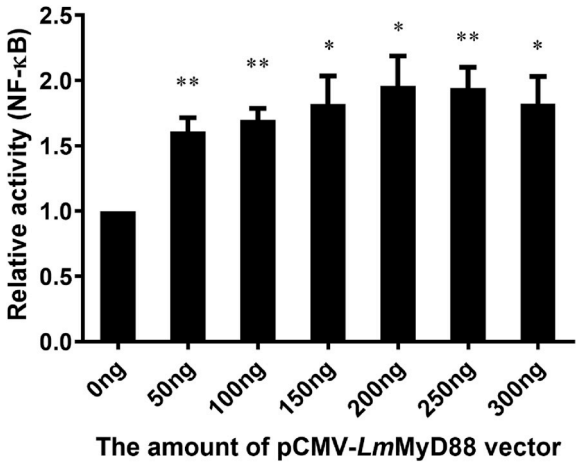

Fig. 7. Effect of LmMyD88 overexpression on the activity of the *L. morii* NF-κB promoter in HEK293T cells. 7 groups were set up and each group was transfected with pCMV-LmMyD88 0 (control group), 50, 100, 150, 200, 250, and 300 ng. The transgenic amount of the *L. morii* NF-κB promoter was 100 ng phRL-TK was used as the reference plasmid. *Represents a significant difference from the control group (n = 3, *P < 0.05, **P < 0.01).

the innate immune response by MyD88-dependent pathway. The results showed that the relative constitutive expression of MyD88 was higher in the kidney of adults. After 24 h of infection with *P. aeruginosa*, the expression of MyD88 in the kidney was significantly increased. After 12 h of *P. aeruginosa* infection, the expression of MyD88 in the gill also increased significantly, which was in direct contact with the living environment. The results showed that *P. aeruginosa* infection induced the expression of LmMyD88.

The results of LmMyD88 localization showed that LmMyD88 clustered in the cells. Specifically, LmMyD88 was localized in both the nucleus and cytoplasm. While LmMyD88 was distributed in mitochondria and endoplasmic reticulum, it was not specifically present in these organelles. The result was roughly the same as the predicted results of protein localization. The morphology of LmMyD88 in cells was similar to that of *Danio rerio* MyD88, and all of them were condensed into clusters [32]. Similarly, mammalian MyD88 aggregates into various shapes in cells [33]. It can be seen that LmMyD88, like other vertebrate MyD88, exists in condensed form in the cells, but it is not specifically located in endoplasmic reticulum and mitochondria.

The typical MyD88-dependent pathway activates the nuclear transcription factor NF-κB, prompting the NF-κB into the nucleus and the subsequent generation of inflammatory cytokines. *Paralichthys olivaceus* TLR7/8 signaling pathway study confirmed that the inhibition of MyD88 activation can significantly reduce the activity of NF-κB [34]. Similarly, through targeting MyD88, studies in *Miiuy croaker* restrained the activity of NF-κB, thus inhibiting the production of inflammatory cytokines and avoiding excessive inflammation [35]. In this study, LmMyD88 overexpression in cells confirmed that LmMyD88 enhanced the activity of NF-κB promoter downstream of the TLR signaling pathway. These results indicated that LmMyD88 activated NF-κB, which was typical of the MyD88 in other species.

This study identified the ORF sequence of the LmMyD88 had the DD and TIR domain of a typical MyD88 with multiple conserved regions but had a certain specificity in amino acid arrangement compared with mammals and fish. LmMyD88 was expressed in multiple tissues of the Northeast Chinese lamprey, and was induced to express after *P.*

aeruginosa infection. It is suggested that LmMyD88 may be involved in the bacterial-induced innate immune response. The existential state of LmMyD88 in cells was similar to that of fish. The dual luciferase reporter gene assay showed that LmMyD88 had an association with the downstream nuclear transcription factor NF-κB, like a typical MyD88. Previous studies showed that MyD88 had more diverse functions in other vertebrates. For example, in *Danio rerio*, MyD88 can synergistically activate IFN-β with IFN regulatory factor [36], speculating that LmMyD88 may have other functions in the TLR signaling pathway of *L. morii* like MyD88 in higher vertebrates. Consider the results so far, whether LmMyD88 affects the NF-κB signaling pathway by recruiting and interacting with IRAK4? Whether LmMyD88 can activate interferon in *L. morii*? These questions which may reveal the similarities and divergences between the biological function of LmMyD88 and that of higher vertebrates need further research.

Acknowledgments

This work was supported by Scientific Research Foundation for the Returned Overseas Chinese Scholars, State Education Ministry (D-8002-15-0042), the China-US Ocean Research Center Fund (A1-0209-15-0806), the Shanghai First-Class Discipline Construction Fund and the National Natural Science Foundation of China (No. 31501166), the Shanghai Municipal Education Commission Aquatic Peak Program.

Appendix A. Supplementary data

Supplementary data to this article can be found online at https://doi.org/10.1016/j.fsi.2019.09.035.

References

[1] S. Akira, S. Uematsu, O. Takeuchi, Pathogen recognition and innate immunity, Cell 124 (4) (2006) 783–801.
[2] S. Akira, H. Hemmi, Recognition of pathogen-associated molecular patterns by TLR family, Immunol. Lett. 85 (2) (2003) 85–95.
[3] K. Takeda, S. Akira, Toll-like receptors in innate immunity, Int. Immunol. 17 (1) (2005) 1–14.
[4] J.L. Casanova, L. Abel, L. Quintana-Murci, Human TLRs and IL-1Rs in host defense: natural insights from evolutionary, epidemiological, and clinical genetics, Annu. Rev. Immunol. 29 (2011) 447–491.
[5] T. Hirotani, M. Yamamoto, Y. Kumagai, S. Uematsu, I. Kawase, O. Takeuchi, S. Akira, Regulation of lipopolysaccharide-inducible genes by MyD88 and Toll/IL-1 domain containing adaptor inducing IFN-beta, Biochem. Biophys. Res. Commun. 328 (2) (2005) 383–392.
[6] C. Couillault, N. Pujol, J. Reboul, L. Sabatier, J.F. Guichou, Y. Kohara, J.J. Ewbank, TLR-independent control of innate immunity in Caenorhabditis elegans by the TIR domain adaptor protein TIR-1, an ortholog of human SARM, Nat. Immunol. 5 (5) (2004) 488–494.
[7] L.A. O'Neill, A.G. Bowie, The family of five: TIR-domain-containing adaptors in Toll-like receptor signalling, Nat. Rev. Immunol. 7 (5) (2007) 353–364.
[8] T. Kawai, S. Akira, The role of pattern-recognition receptors in innate immunity: update on Toll-like receptors, Nat. Immunol. 11 (5) (2010) 373–384.
[9] K.A. Lord, B. Hoffman-Liebermann, D.A. Liebermann, Nucleotide sequence and expression of a cDNA encoding MyD88, a novel myeloid differentiation primary response gene induced by IL6, Oncogene 5 (7) (1990) 1095–1097.
[10] T. Kaisho, S. Akira, Toll-like receptor function and signaling, J. Allergy Clin. Immunol. 117 (5) (2006) 979–987 quiz 988.
[11] N. Suzuki, S. Suzuki, G.S. Duncan, D.G. Millar, T. Wada, C. Mirtsos, H. Takada, A. Wakeham, A. Itie, S. Li, J.M. Penninger, H. Wesche, P.S. Ohashi, T.W. Mak, W.C. Yeh, Severe impairment of interleukin-1 and Toll-like receptor signalling in mice lacking IRAK-4, Nature 416 (6882) (2002) 750–756.
[12] T.P. Bonnert, K.E. Garka, P. Parnet, G. Sonoda, J.R. Testa, J.E. Sims, The cloning and characterization of human MyD88: a member of an IL-1 receptor related family, FEBS Lett. 402 (1) (1997) 81–84.
[13] S. Wheaton, M.D. Lambourne, A.J. Sarson, J.T. Brisbin, A. Mayameei, S. Sharif, Molecular cloning and expression analysis of chicken MyD88 and TRIF genes, DNA Seq 18 (6) (2007) 480–486.
[14] C. Prothmann, N.J. Armstrong, R.A. Rupp, The Toll IL-1 receptor binding protein MyD88 is required for (Xenopus laexis) formation, Chem. Dev. 97 (2000) 85–92.
[15] C. Jault, L. Pichon, J. Chluba, Toll-like receptor gene family and TIR-domain adapters in Danio rerio, Mol. Immunol. 40 (11) (2004) 759–771.
[16] Z.X. Zhou, B.C. Zhang, L. Sun, Poly(I:C) induces antiviral immune responses in Japanese flounder (Paralichthys olivaceus) that require TLR3 and MDA5 and is negatively regulated by Myd88, PLoS One 9 (11) (2014) e112918.
[17] A. Rebl, T. Goldammer, U. Fischer, B. Kollner, H.M. Seyfert, Characterization of two key molecules of teleost innate immunity from rainbow trout (Oncorhynchus mykiss): MyD88 and SAA, Vet. Immunol. Immunopathol. 131 (1–2) (2009) 122–126.
[18] I. Skjaeveland, D.B. Iliev, G. Strandskog, J.B. Jorgensen, Identification and characterization of TLR8 and MyD88 homologs in Atlantic salmon (Salmo salar), Dev. Comp. Immunol. 33 (9) (2009) 1011–1017.
[19] D. Tang, Y. Gao, R. Wang, Y. Sun, T. Xu, Characterization, genomic organization, and expression profiles of MyD88, a key adaptor molecule in the TLR signaling pathways in miiuy croaker (Miichthys miiuy), Fish Physiol. Biochem. 38 (6) (2012) 1667–1677.
[20] P. Janvier, Palaeontology: modern look for ancient lamprey, Nature 443 (7114) (2006) 921–924.
[21] J. Kasamatsu, H. Oshiumi, M. Matsumoto, M. Kasahara, T. Seya, Phylogenetic and expression analysis of lamprey toll-like receptors, Dev. Comp. Immunol. 34 (8) (2010) 855–865.
[22] P. Su, X. Liu, Y. Han, Z. Zheng, G. Liu, J. Li, Q. Li, Identification and characterization of a novel IkappaB-epsilon-like gene from lamprey (Lampetra japonica) with a role in immune response, Fish Shellfish Immunol. 35 (4) (2013) 1146–1154.
[23] J.L. Slack, K. Schooley, T.P. Bonnert, J.L. Mitcham, E.E. Qwarnstrom, J.E. Sims, S.K. Dower, Identification of two major sites in the type I interleukin-1 receptor cytoplasmic region responsible for coupling to pro-inflammatory signaling pathways, J. Biol. Chem. 275 (7) (2000) 4670–4678.
[24] M. Loiarro, G. Gallo, N. Fanto, R. De Santis, P. Carminati, V. Ruggiero, C. Sette, Identification of critical residues of the MyD88 death domain involved in the recruitment of downstream kinases, J. Biol. Chem. 284 (41) (2009) 28093–28103.
[25] Y.W. Li, Z. Wang, Z.Q. Mo, X. Li, X.C. Luo, X.M. Dan, A.X. Li, Grouper (Epinephelus coioides) MyD88 and Tollip: intracellular localization and signal transduction function, Fish Shellfish Immunol. 42 (1) (2015) 153–158.
[26] L. Yu, L. Zhang, H. Yang, G. Gui, Y. Liu, Y. Xiao, Identification and characterization of the myeloid differentiation factor 88 gene in yellow catfish, 3 Biotech 8 (10) (2018) 430.
[27] Y. Cheng, H. Wang, Y. Yan, C. Ding, J. Sun, Two myeloid differentiation factor 88 (MyD88) isoforms identified in ducks, Dev. Comp. Immunol. 52 (2) (2015) 144–154.
[28] L. Huo, M. Bao, Z. Lv, C. Chi, T. Wang, H. Liu, Identification, functional characterization and expression pattern of myeloid differentiation factor 88 (MyD88) in Sepiella japonica, Fish Shellfish Immunol. 79 (2018) 112–119.
[29] X. Ning, R. Wang, X. Li, S. Wang, M. Zhang, Q. Xing, Y. Sun, S. Wang, L. Zhang, X. Hu, Z. Bao, Genome-wide identification and characterization of five MyD88 duplication genes in Yesso scallop (Patinopecten yessoensis) and expression changes in response to bacterial challenge, Fish Shellfish Immunol. 46 (2) (2015) 181–191.
[30] T. Qin, X. Zhao, H. Luan, H. Ba, L. Yang, Z. Li, L. Hou, X. Zou, Identification, expression pattern and functional characterization of As-MyD88 in bacteria challenge and during different developmental stages of Artemia sinica, Dev. Comp. Immunol. 50 (1) (2015) 9–18.
[31] W.S. Huang, Z.X. Wang, Y. Liang, P. Nie, B. Huang, Characterization of MyD88 in Japanese eel, Anguilla japonica, Fish Shellfish Immunol. 81 (2018) 374–382.
[32] Y. Liu, M. Li, S. Fan, Y. Lin, B. Lin, F. Luo, C. Zhang, S. Chen, Y. Li, A. Xu, A unique feature of Toll/IL-1 receptor domain-containing adaptor protein is partially responsible for lipopolysaccharide insensitivity in zebrafish with a highly conserved function of MyD88, J. Immunol. 185 (6) (2010) 3391–3400.
[33] T. Nishiya, E. Kajita, T. Horinouchi, A. Nishimoto, S. Miwa, Distinct roles of TIR and non-TIR regions in the subcellular localization and signaling properties of MyD88, FEBS Lett. 581 (17) (2007) 3223–3229.
[34] Z.X. Zhou, L. Sun, Immune effects of R848: evidences that suggest an essential role of TLR7/8-induced, Myd88- and NF-kappaB-dependent signaling in the antiviral immunity of Japanese flounder (Paralichthys olivaceus), Dev. Comp. Immunol. 49 (1) (2015) 113–120.
[35] Q. Chu, Y. Sun, J. Cui, T. Xu, Inducible microRNA-214 contributes to the suppression of NF-kappaB-mediated inflammatory response via targeting myd88 gene in fish, J. Biol. Chem. 292 (13) (2017) 5282–5290.
[36] H. Feng, Y.B. Zhang, Q.M. Zhang, Z. Li, Q.Y. Zhang, J.F. Gui, Zebrafish IRF1 regulates IFN antiviral response through binding to IFNvarphi1 and IFNvarphi3 promoters downstream of MyD88 signaling, J. Immunol. 194 (3) (2015) 1225–1238.